Paper ID:

Flow-Induced Vibration of an Inelastic Cylinder in Wake

Jian Liu and Md. Mahbub Alam*
Mechanical and Automation Engineering Department
Harbin Institute of Technology (Shenzhen), Shenzhen 518055, China
E-mail: alamm28@yahoo.com; alam@hit.edu.cn

Abstract

Generally, elasticity or stable equilibrium of a structure is a requirement for vibration generation. Is it true for a structure undergoing fluid flow? A systematic study is conducted on the wake-induced vibration of an inelastic or zero structural stiffness cylinder placed behind a perfectly elastic or rigid cylinder. The mass ratio m of the inelastic cylinder is 11.1. The inelastic cylinder in the wake becomes aerodynamically elastic because of the flow-induced stiffness generated. Consequently, galloping vibrations appear, influenced by the quiescent fluid added mass, damping, and flow-induced stiffness. The flow-induced stiffness exhibits a linear relationship with the Reynolds number, varying between the reattachment and coshedding flow regimes, as well as between the desynchronization and galloping branches. Notably, this stiffness is generally greater in the reattachment regime than the coshedding regime and decreases during the galloping branch compared to the desynchronization branch.*

Keywords: inelastic cylinder, stiffness, flow-induced vibration, galloping, structure.

1. Introduction

Flow around a circular cylinder is one of the classical problems in fluid mechanics. An exclusive feature of the flow phenomena is that an isolated circular cylinder subjected to flow undergoes vortex-induced vibration (VIV). Many studies have been conducted on the VIV mechanism of a circular cylinder [1–3]. The VIV range and the maximum vibration amplitude in the VIV depend on several independent parameters including the cylinder mass ratio (m^*), damping ratio (ζ), and Reynolds number (Re, based on the cylinder diameter D and freestream velocity U_∞). Two parallel cylinders are commonly considered the simplest configuration or model to comprehend the underlying flow physics involved in a cylinder array.

Previous works revealed that an elastic cylinder placed in the wake of a rigid cylinder experiences wake-induced galloping vibration [4]. Wake-induced vibration responses are characterized by increasing, large-amplitude vibrations at high reduced velocities, where the vortex shedding frequency is higher than the cylinder oscillation frequency. The phenomenon is, therefore, distinct from VIV. Assi et al. [4] experimentally investigated the wake-induced vibrations of a pair of cylinders in tandem arrangements at $L/D = 4 - 20$, $m^* = 2.6$, $Re = 3 \times 10^3 - 2.5 \times 10^4$, where L is the center-to-center distance between the two cylinders (Fig. 1c). They revealed that wake-induced vibrations of the downstream cylinder in the coshedding flow regime are excited by the unsteady vortex-structure interactions between the downstream- and upstream-cylinder wakes, where coherent vortices interfering with the downstream cylinder induce the instability and force fluctuation to generate wake-induced vibrations [5]. For the reattachment flow regime, the gap shear layers play the same role in the wake-induced vibrations [6, 7].

Hu et al. [8] made a wind tunnel test, investigating the cross-flow vibrations of two tandem cylinders at $L/D = 1.2 - 8.0$, $m^* = 268.9$, $Re = 4 \times 10^3 - 4.2 \times 10^4$. Three regimes of vibrations are identified and classified based on L/D.

Structural stiffness is a characteristic parameter defining the natural frequency of the structure. Its value may vary between the two extremities of zero (completely inelastic structure) and infinite (infinitely rigid, fixed structure). These two extremities cover the possible ranges of the reduced velocity, with the zero and infinite stiffnesses corresponding to the infinite and zero reduced velocities, respectively. There are several studies on the two fixed (zero reduced velocity) cylinders. However, limited attention has been paid to the vibration of an inelastic cylinder (zero structural stiffness). Generally, a system must be of stable equilibrium (minimum potential energy) to undergo oscillation under a disturbance or plucking. A system without stiffness is said to be in neutral equilibrium (zero or constant potential energy) and hence does not meet the vibration requirement.

This work aims at a comprehensive experiment, focusing on characterizing the vibration response, frequency response, flow-induced stiffness, fluid force, and their dependence on Re and L/D covering both reattachment and

coshedding flow regimes. We considered a simple case of two circular cylinders where the downstream cylinder is of zero stiffness, and the upstream cylinder is of infinite stiffness (rigid). The zero stiffness of the downstream cylinder is succeeded by letting the cylinder move freely in the cross-flow direction without employing any springs.

2. Experimental methodology

Experiments were carried out in a free-surface, low-speed recirculating water channel with a test section of 2.4 m in length, 0.3 m in width, and 0.6 m in height. Figure 1 displays sketches of the experimental setup and symbol definitions. The setup of the cylinder vibration was placed on the top of the test section. The two cylinders – each of diameter D – were attached to this setup and suspended vertically into the channel (Fig. 1a, b). They were positioned in tandem along the vertical midplane of the test section. The L is the streamwise separation between the cylinders, and U_∞ is the freestream velocity measured by a pitot tube placed at (x/D, y/D) = (−65, 4) on the midspan plane, with x and y representing the streamwise and cross-stream coordinate axes (Fig. 1c). The upstream cylinder was rigidly attached to the fixed supports restricting the cylinder movement in any direction. The upper end of the downstream cylinder was connected to a load cell fixed on two air bearings (Fig. 1a, b). They were installed on two parallel stainless-steel shafts, respectively, allowing the movement of the air bearings, hence of the cylinder, in the transverse direction only.

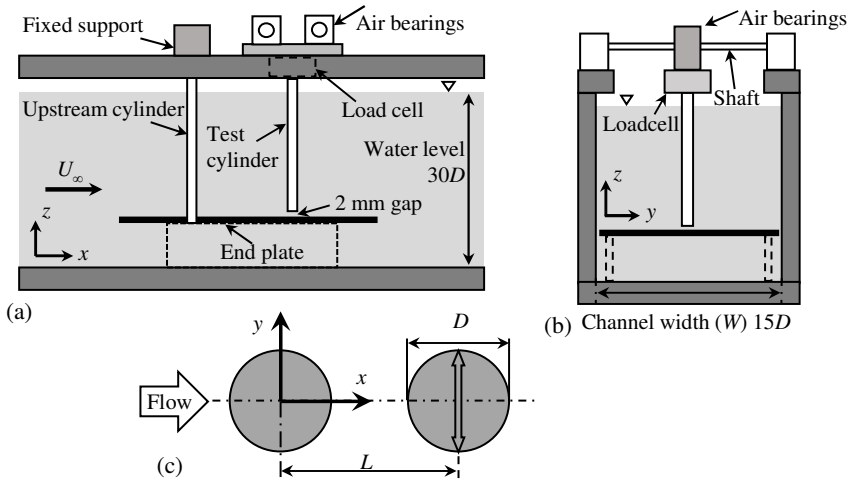


Fig. 1. (a) Experimental setup, (b) front view of the setup, and (c) definitions of symbols.

The L/D was systematically varied as L/D = 2.0, 2.5, 3.0, 3.5, 4.0, 4.5, 5.0, 5.5 and 6.0. The total moving mass of the cylinder system was m = 1132 g and the displaced water mass by the cylinder was $m_d = \rho\pi D^2 l/4 = 102$ g, giving a mass ratio $m^* = m/m_d = 11.1$, where l is the cylinder length immersed in water. The cylinder displacement Y was measured using a laser vibrometer (OFV-505/5000, Polytec) having a resolution of 0.05 μm. The U_∞ was varied from 0.098 m/s to 0.591 m/s, corresponding to $Re = 1.97 \times 10^3 - 1.18 \times 10^4$.

A load cell (K3D60a, ME) was positioned between the cylinder and air bearings for measuring hydrodynamic forces exerted on the cylinder. The loadcell signal was amplified by an amplifier (GSV-1A4 SubD37, ME) with a cut-off frequency of 250 Hz. Both laser vibrometer and loadcell outputs were digitized with a 16-channel A/D board at a sampling frequency of 1.5k Hz for a sampling duration of 100 s. The oscillation frequency f_o and vortex shedding frequency f_v of the cylinder were determined from the power spectral density function E_Y of Y and E_{C_L} of lift force C_L, respectively, using a fast Fourier transform algorithm.

The structural attributes of an elastic structure are generally mass, stiffness, and damping, which inherently characterize the system. The equation of motion of a cylinder oscillating in the y (transverse) direction is

$$m\ddot{Y}(t) + c\dot{Y}(t) + kY(t) = F_L(t), \tag{1}$$

where m is the total oscillating mass, c is the structural damping, k is the spring stiffness, and $F_L(t)$ is the lift force. The Y, $\dot{Y}$, and $\ddot{Y}$ are the displacement, velocity, and acceleration of the cylinder, respectively. The $Y = 0$ defines the equilibrium position of the cylinder. The $F_L(t)$ on the cylinder is calculated by subtracting the net inertia force from the net force measured by the load cell. The net inertia force is the cylinder acceleration times submerged cylinder mass plus displaced fluid mass [10]. The $Y(t)$ and $F_L(t)$ can be assumed harmonic [2, 10]:

$$Y(t) = Y_0 \sin \omega t \,, \quad \text{and} \quad F_L(t) = F_{L0} \sin(\omega t + \phi) \,, \tag{2}$$

where Y_0 is the amplitude of the cylinder oscillation, F_{L0} is the amplitude of the lift force, and ϕ is the phase lag between the lift force and cylinder displacement. The ϕ is a crucial parameter, determining the sign of energy transfer from the fluid to the body motion and *vice versa* [10, 11]. In this work, the structural stiffness of the downstream cylinder is made zero (i.e., $k = 0$, no spring) by allowing the cylinder to move freely, using air bearing, in the transverse direction.

3. Vibration responses

A cylinder mounted on air bearings without springs can be considered inelastic, with zero stiffness and zero natural frequency. Here, we present results for the inelastic cylinder placed in the wake of a fixed cylinder (Fig. 1). Since the cylinder has a zero natural frequency, the freestream flow velocity cannot be normalized to U_r but to *Re*. The amplitude *A* of the cylinder vibration was calculated by measuring the root-mean-square value of the displacement and multiplying by $\sqrt{2}$. Figure 2(a–c) shows dependencies of *A/D* on *Re* (= 1.97 × 10^3 – 1.18 × 10^4) and *L/D* (= 2.0 – 6.0). The cylinder undergoes large amplitude vibrations once the *Re* is sufficiently high, depending on *L/D*. At *L/D* = 2.0, 2.5, and 3.0, violent vibrations prevail at *Re* > 8.3 × 10^3, 6.7 × 10^3 and 6.7 × 10^3, respectively (Fig. 3a). Here the small-amplitude vibrations (*Re* < 8.3 × 10^3, 6.7 × 10^3 and 6.7 × 10^3 for *L/D* = 2.0, 2.5, and 3.0, respectively) are defined as the desynchronization branch (DB) while the large-amplitude vibrations (*Re* > 8.3 × 10^3, 6.7 × 10^3 and 6.7 × 10^3 for *L/D* = 2.0, 2.5, and 3.0, respectively) as the galloping branch (GB).

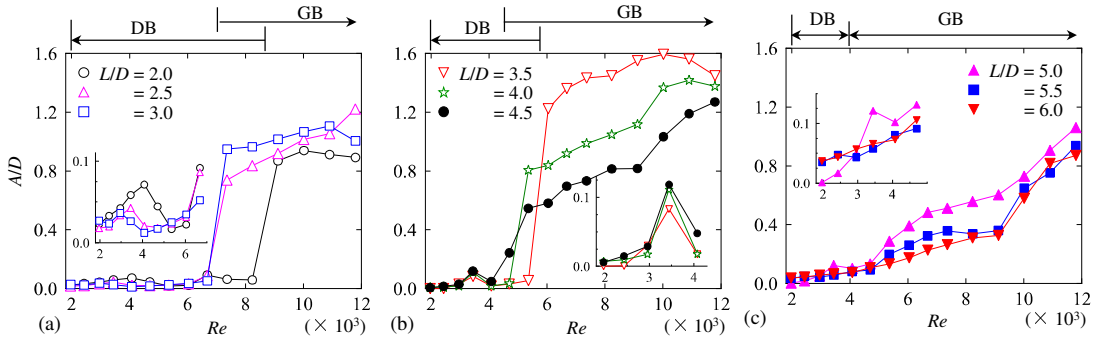


Fig. 2. (a–c) Dependence of vibration amplitude *A*/*D* on *Re* and *L*/*D*.

The onset of the violent vibrations is characterized by jumps in *A/D* from *A/D* ~ 0.05 to 0.7–0.9 depending on *L/D*. Similar observations are made for *L/D* = 3.5, 4.0, and 4.5, albeit with some distinct features (Fig. 2b). First, a small peak is observed at *Re* = 3.6 × 10^3 in the DB, with the peak value being slightly larger than that for *L/D* ≤ 3.0 in Fig. 2(a). Second, the *Re* values at the onsets of vibrations are smaller than those for *L/D* ≤ 3.0. The jump in *A/D* ranges from *A/D* ~ 0.05 to 1.2 depending on *L/D*. The *A/D* in the GB levels off earlier for *L/D* = 2.0 and 3.0 than for *L/D* = 2.5, 3.5, 4.0 and 4.5.

The *A/D* dependencies on *L/D* = 5.0 – 6.0 are qualitatively similar to each other (Fig. 2c) but different from those on *L/D* ≤ 4.5 (Fig. 2a, b). The jump in *A/D* becomes faint, and the onsets of GB prevail at small *Re*. The *A/D* in the GB generally increases with *Re* but decreases with increasing *L/D* from 5.0 to 6.0. Overall, the *A/D* is largest at *L/D* = 2.5 in the reattachment flow regime and at *L/D* = 3.5 in the coshedding flow regime where *A/D* declines with increasing *L/D* from 3.5 to 6.0.

4. Effective natural frequency and vortex shedding frequency

Here the cylinder oscillation frequency is referred to as the effective natural frequency f_w of the cylinder undergoing the induced stiffness (effective stiffness). The vortex shedding frequency f_v and f_w – identified from the power spectra of fluctuating lift and cylinder displacement, respectively, – characterize and distinguish the flow-induced vibrations. Figure 3(a–c) presents variations in the corresponding Strouhal numbers St_v (= $f_v D/U_\infty$) and St_w (= $f_w D/U_\infty$) with *Re* for various *L/D* values. The St_w is smaller than St_v for all the *Re* and *L/D* values examined. The St_w with increasing *Re* generally decreases from 0.063 – 0.079 at *Re* = 1.97 × 10^3 to 0.028 – 0.032 at *Re* = 1.18 × 10^4 depending on *L/D*. The decrease with *Re* is rather mild in the GB than in the DB. Although *Re* influences St_w for all *L/D* values, the *Re* effect on St_w is more palpable in the reattachment flow regime (*L/D* ≤ 3.0)

than in the coshedding flow regime ($L/D \geq 3.5$). Similarly, L/D predominantly affects St_w for $L/D \leq 3.0$, but not much for $L/D \geq 3.5$.

The St_v displays a small peak at $2 \times 10^3 < Re < 6 \times 10^3$ (depending on L/D) and a jump at $4 \times 10^3 < Re < 7 \times 10^3$ (depending on L/D) for $L/D = 2.0 - 4.5$. The occurrence of the peaks in St_v corresponds to the small peaks in A/D (see the insets in Fig. 2). The jump takes place at the onset of the violent vibration and is hence associated with the large amplitude oscillation of the cylinder except for the smallest $L/D = 2.0$ where St_v gradually waxes to 0.217 at $Re = 5.36 \times 10^3$ and then wanes to 0.149 at $Re = 1.18 \times 10^4$. In the GB (beyond the jump), St_v wanes with Re for $L/D \leq 3.0$ (reattachment flow) but more or less constant for $L/D \geq 3.5$ (coshedding flow).

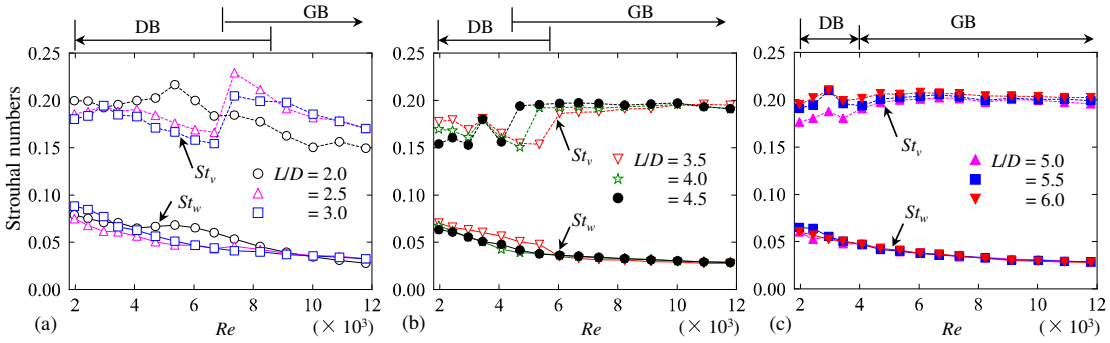


Fig. 3. (a–c) Dependence of Strouhal numbers St_v (dashed lines) and St_w (solid slines) on Re and L/D.

5. Flow-induced effective stiffness k_e

The cylinder exhibits flow-induced vibrations in the absence of springs (zero structural stiffness). Since there is no physical stiffness in the system, the only way of having the stiffness is the flow-induced effective stiffness resulting from wake- and motion-induced lift force generated on the cylinder to sustain the cylinder motion. When ϕ is the phase lag between the lift force and displacement, the lift force can be expressed as

$$F_{L0}\sin(\omega t+\phi) = F_{L0}\cos\phi\sin\omega t + F_{L0}\sin\phi\cos\omega t, \tag{3}$$

where the first and second terms on the right-hand side are force components inphase with the cylinder displacement and velocity, respectively. Eq. (1) can, therefore, be written as

$$m\ddot{Y} + (c - \frac{F_{L0}\sin\phi}{\omega Y_0})\dot{Y} + (k - \frac{F_{L0}\cos\phi}{Y_0})Y = 0. \tag{4}$$

Eq. (4) reflects that $-\frac{F_{L0}\sin\phi}{\omega Y_0}$ is the flow-induced effective damping c_e and $-\frac{F_{L0}\cos\phi}{Y_0}$ is the flow-induced effective stiffness k_e, both resulting from fluid-structure interactions. We can, therefore, write

$$c_e = -\frac{F_{L0}\sin\phi}{\omega Y_0} \text{ and } k_e = -\frac{F_{L0}\cos\phi}{Y_0}. \tag{5a, b}$$

Interestingly, k_e is determined by the ratio of F_{L0} and Y_0, while ϕ must be greater than 90° for k_e to be positive. Now, the effective stiffness can be rewritten as an integral term associated with Y,

$$k_e = -\frac{2}{nTY_0^2}\int_t^{t+nT} F_L Y dt', \tag{6}$$

where T is the oscillation period, and n is the number of periods considered for the integration.

The k_e, being a function of Re and L/D, describes the flow-induced effective restoring force proportional to the displacement. The above equations are admissible for sinusoidal motion at a single frequency. The F_L and Y/D signals both contain two frequencies: the cylinder oscillation frequency and vortex shedding frequency. The corresponding stiffnesses k_{ew} and k_{ev} were calculated from the low- and high-pass filtered signals of F_L and Y/D. Figure 4(a–c) presents the dependence of k_{ew} on Re and L/D. The k_{ew} generally grows linearly with Re, except for $L/D = 2.0 - 3.5$ where the shear layer reattachment, detachment, and switch are involved. At $L/D = 2.0$, the k_{ew} linearly increases to a peak of 40.7 at $Re = 6.7 \times 10^3$ before linearly declining. The behavior of k_{ew} at $L/D \geq 3.5$ (coshedding regime) is different from that at $L/D = 2.0 - 3.0$. For $L/D \geq 3.5$, k_{ew} generally increases with Re because of a large increase in lift amplitude (not shown), overwhelming the increase of A/D. A break in the linear

change in k_{ew} is identified at Re = 5.7 × 10^3 for L/D = 3.5, which is a footprint of the transmutation of the reattachment flow to the coshedding flow.

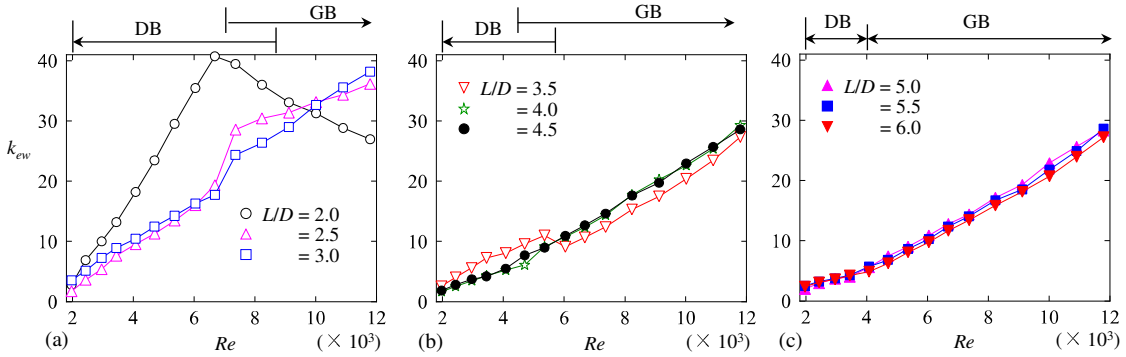


Fig. 4. (a–c) Dependence on Re and L/D of added stiffness k_{ew} associated with the vibration frequency.

6. Role of flow-induced effective stiffness in determining vibration frequency

As observed in Fig. 3, St_w declines with increasing Re and the declination is sensitive to both L/D and GB (i.e., Re). To press home the insight into the relationship of St_w with L/D and Re, St_w could be shown as a function of Re while the natural frequency f_{nw} associated with k_{ew} and corresponding reduced velocity U_{rw} are:

$$St_w = \frac{f_w D}{U_\infty} = \frac{f_w \rho D^2 / \mu}{Re} \quad \text{and} \quad f_{nw} = \frac{1}{2\pi}\sqrt{k_{ew}/m}, \quad \text{and} \tag{7}$$

$$U_{rw} = \frac{U_\infty}{f_{nw} D} = \frac{2\pi U_\infty}{D\sqrt{k_{ew}/m}} = \frac{2\pi\rho U_\infty D/\mu}{\rho D^2\sqrt{k_{ew}/m}/\mu} = \frac{2\pi\mu Re}{\rho D^2\sqrt{k_{ew}/m}}. \tag{8}$$

Note that St_w is estimated from the power spectrum of the directly measured displacement signal while U_{rw} and f_{nw} are estimated from the fluid stiffness k_{ew}. Multiplying eq. (7) with eq. (8), we can obtain

$$St_w \times U_{rw} = \frac{2\pi f_w}{\sqrt{k_{ew}/m}} = \frac{f_w}{f_{nw}}. \tag{9}$$

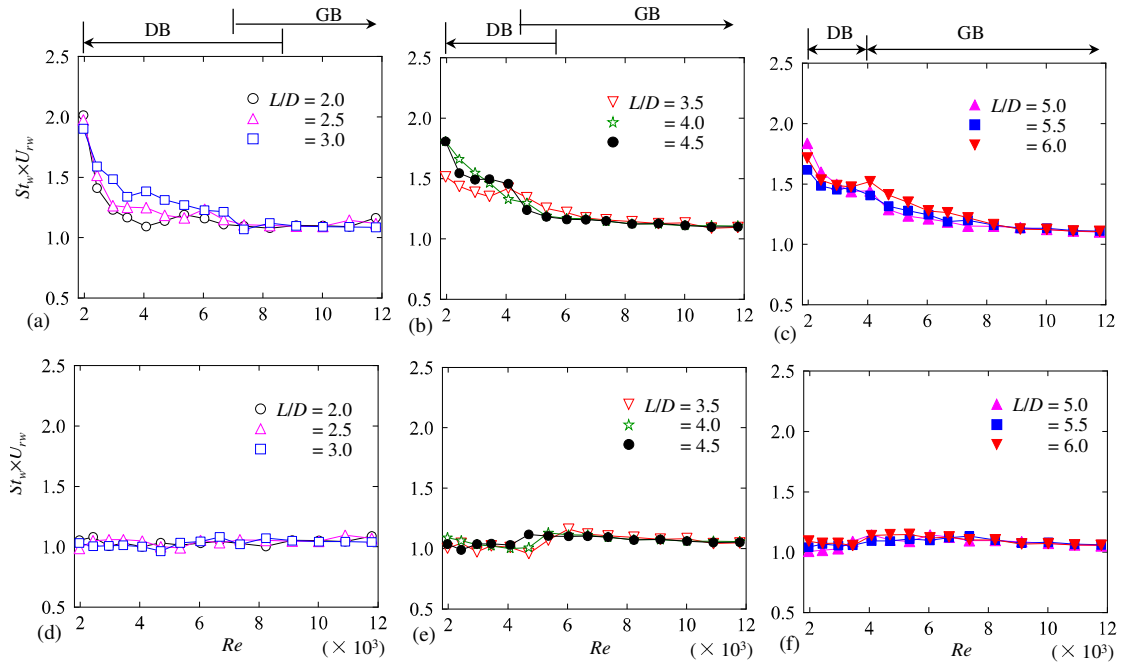


Fig. 5. Dependence on Re and L/D of $St_w \times U_{rw}$: (a–c) when only k_{ew} is considered in U_{rw}, (d–f) when k_{ew}, m_d and c_{cv} are all considered U_{rw}.

The $St_w \times U_{rw}$ essentially represents the ratio of directly measured oscillation frequency and estimated natural frequency associated with the flow-induced effective stiffness. Figure 5(a–c) presents the variations of $St_w \times U_{rw}$ with *L/D* and *Re*. It is observed that $St_w \times U_{rw}$ is greater than 1.0 and generally decreases with *Re* in the DB while approaching 1.0 in the GB for all *L/D* values examined. The results indicate that the oscillation frequency in the GB is the same as the natural frequency associated with the effective stiffness caused by the flow. In the DB, $St_w \times U_{rw} > 1.0$ implies $f_w > f_{nw}$ where the quiescent-fluid added mass and damping c_{cv} play a role in modifying f_{nw} as k_{ew} is small. For a circular cylinder, the quiescent fluid added mass equals the displaced fluid mass m_d by the cylinder. Taking m_d and c_{cv} into account in the calculation of f_{nw}, we can obtain

$$f_{nw} = \frac{1}{2\pi}\sqrt{\frac{k_{ew}}{m+m_d} + \frac{c_{cv}\dot{Y}_0}{(m+m_d)Y_o}} = \frac{1}{2\pi}\sqrt{\frac{k_{ew}}{m+m_d} + \frac{4F_c}{\pi(m+m_d)Y_0}}\,. \tag{10}$$

Now f_{nw} involves m_d, F_c and Y_0. Eq. (10) reflects that m_d and F_c may have a greater role in f_{nw} when k_{ew} and Y_0 are small (i.e. in the DB) while their role is negligible when k_{ew} and/or Y_0 are large (i.e. in GB). Considering f_{nw} in Eq. (10), $St_w \times U_{rw}$ is recalculated and presented in Fig. 5(d–f). Now all $St_w \times U_{rw}$ data collapse into 1.0 for all *Re* and *L/D* values, regardless of small or large amplitude vibrations. This further substantiates that m_d and F_c can modify f_{nw} for a small k_{ew} and Y_0 but not for a large k_{ew} and Y_0. The collapse of $St_w \times U_{rw}$ data into 1.0 proves $f_w = f_{nw}$, i.e., the cylinder oscillation occurs at the aerodynamic natural frequency corresponding to the aerodynamic stiffness.

7. Conclusions

A structurally inelastic cylinder placed behind another elastic cylinder becomes aerodynamically elastic, yielding a finite natural frequency. The ensuing stiffness is proportional to the ratio of the lift force F_{L0} to cylinder displacement Y_0. The k_{ew} linearly grows with increasing *Re*. with a large increase in the coshedding regime than in the reattachment regime. The aerodynamic elasticity of the inelastic cylinder may incur a galloping. The inelastic cylinder for the *L/D* range examined undergoes small-amplitude vibration for small *Re* in the desynchronized branch (DB) since vortex shedding is desynchronized from the natural vibration of the inelastic cylinder. The vortex shedding frequency St_v is always larger than the cylinder oscillation frequency St_w, and vortex shedding is not locked in with the cylinder oscillation, irrespective of *Re* and *L/D*. With increasing *Re*, St_w declines rapidly in the DB but mildly in the GB. The quiescent fluid added mass and Coulomb damping both play a role in determining St_w at small *Re* where k_{ew} is small. Furthermore, St_w is dependent on *L/D* in the reattachment regime but not in the coshedding regime. The predominant cylinder oscillation takes place at the natural frequency St_{nw} of the inelastic cylinder, i.e., $St_w = St_{nw}$, regardless of *Re* and *L/D*. This is confirmed by the collapsed $St_w \times U_{rw}$ data around 1.0, indicating the cylinder oscillation at its aerodynamic natural frequency, for all *Re* and *L/D* values, when the quiescent fluid added mass m_d, Coulomb damping c_{cv}, and k_{ew} are considered in the estimation of f_{nw}. The effect of m_d and c_{cv} on f_{nw} is not negligible when *A/D* and k_{ew} are small but can be neglected otherwise.

8. References

[1] C.C., Feng, "The measurement of vortex induced effects in flow past stationary and oscillating circular and D-section cylinders", Masters thesis, University of British Columbia, BC, Canada, 1968.

[2] T.L. Morse, and C.H.K. Williamson, "Fluid forcing, wake modes, and transitions for a cylinder undergoing controlled oscillations" *J. Fluids Struct.* **25**, 697–712, 2009.

[3] R. Mishra, A. Soti, R. Bhardwaj, S.S. Kulkarni, and M.C. Thompson, "Transverse vortex-induced vibration of a circular cylinder on a viscoelastic support at low Reynolds number", *J. Fluids Struct.* **95**, 102997, 2020.

[4] G.R. Assi, P.W. Bearman, and J.R. Meneghini, "On the wake-induced vibration of tandem circular cylinders: the vortex interaction excitation mechanism", *J. Fluid Mech.* **661**, 365–401, 2010.

[5] M.M. Alam, and J.P. Meyer, "Global aerodynamic instability of twin cylinders in cross flow", *J. Fluids Struct.* **41**, 135–145, 2013.

[6] B. Qin, M.M. Alam, and Y. Zhou, "Two tandem cylinders of different diameters in cross-flow: Flow-induced vibration", *J. Fluid Mech.* **829**, 621–658, 2017.

[7] B. Qin, M.M. Alam, and Y. Zhou, "Free vibrations of two tandem elastically mounted cylinders in crossflow", *J. Fluid Mech.* **861**, 349–381, 2019.

[8] Z Hu, J. Wang, and Y. Sun, "Cross-flow vibrations of two identical elastically mounted cylinders in tandem arrangement using wind tunnel experiment", *Ocean Eng.* **209**, 107501, 2020.

[9] S. Kim, M.M. Alam, and D.K. Maiti, Wake and suppression of flow-induced vibration of a circular cylinder. *Ocean Eng.* **151**, 298–307, 2018.

[10] M.M. Alam, "A note on flow-induced force measurement of oscillating cylinder by loadcell", *Ocean Eng.* **245**, 110538, 2022.

[11] R. Bhatt, & M.M. Alam, "Vibrations of a square cylinder submerged in a wake", *J. Fluid Mech.* **853**, 301–332, 2018.